Lattice Boltzmann formulation for Braginskii magnetohydrodynamics

Paul J. Dellar

OCIAM, Mathematical Institute, 24-29 St Giles', Oxford, OX1 3LB, UK

Abstract

Braginskii magnetohydrodynamics is a single-fluid description of large-scale motions in a strongly magnetised plasma, one in which the ion gyroradius is much smaller than the mean free path between collisions in an unmagnetised plasma of the same density and temperature. The relation between stress and strain rate then becomes highly anisotropic, with the viscous stress being predominantly aligned parallel to the magnetic field lines. We modify an existing lattice Boltzmann formulation of isotropic resistive magnetohydrodynamics to simulate Braginskii magnetohydrodynamics by introducing an anisotropic collision operator for the hydrodynamic distribution functions. This collision operator applies a different relaxation time to the component of stress directed parallel to the magnetic field. The method is illustrated by comparison with independent numerical solutions for steady planar channel flows.

Key words:
lattice Boltzmann methods, matrix collision operators, anisotropic viscosity, plasma physics, magnetohydrodynamics

To appear in *Computers & Fluids* doi:10.1016/j.compfluid.2010.12.004

1. Introduction

Braginskii magnetohydrodynamics (MHD) describes large-scale motions in strongly magnetised plasmas [1, 2, 3, 4]. Charged particles spiral around magnetic field lines due to the Lorentz force, as sketched in figure 1. In a strongly magnetised plasma the typical radius of these spirals, the ion gyroradius, becomes much smaller than the mean free path between collisions. The viscous stress is then directed predominantly along magnetic field lines,

$$\boldsymbol{\Pi}_{\text{visc}} \approx -2\mu_{\parallel}\,\hat{\mathbf{b}}\hat{\mathbf{b}}\,\hat{\mathbf{b}}\hat{\mathbf{b}} : \nabla\mathbf{u}, \tag{1}$$

because the effective mean free path or mixing length in other directions is the gyroradius. Here $\mu_{\parallel}$ is the parallel viscosity, $\mathbf{u}$ the fluid velocity, and $\hat{\mathbf{b}} = \mathbf{B}/|\mathbf{B}|$ a unit vector parallel to the magnetic field $\mathbf{B}$. The colon : denotes a double contraction of the velocity gradient $\nabla\mathbf{u}$ with the tensor $\hat{\mathbf{b}}\hat{\mathbf{b}}$ in dyadic notation [5]. By contrast, standard resistive MHD assumes that the standard isotropic Navier–Stokes form of the viscous stress derived for neutral fluids remains valid. The magnetic field thus only affects the fluid only through a macroscopic Lorentz force.

The Navier–Stokes or other fluid equations, such as Braginskii MHD, do not appear explicitly in the lattice Boltzmann approach to computational fluid dynamics. Instead, fluid equations emerge from the slowly varying limit of a system of linear, constant coefficient hyperbolic equations that describes the motion and interaction of particles in a cut-down version of the kinetic theory of gases in which the particles' velocities are restricted to a discrete set. All nonlinearity is confined to algebraic source terms, making the system very easy to discretise. The resulting explicit, second-order accurate, and readily parallelisable schemes have become very popular in many fields of computational fluid dynamics [6, 7]. The discrete velocity set is typically chosen to be just large enough to recover the isothermal Navier–Stokes equations. Common choices are 9 velocities in two dimensions, as illustrated in figure 2 below, and 15 or 19 velocities in three dimensions. In principle, one may extend the approach into the rarefied regime by using a larger discrete velocity set that reproduces continuous kinetic theory more accurately [8] . However, enlarging the set of discrete velocities usually leads to much poorer numerical stability properties.

In this paper we extend an existing lattice Boltzmann scheme [9] for isotropic resistive MHD to simulate Braginskii MHD. Our approach is similar to the anisotropic scattering matrix used by Care *et al.* [10] in their lattice Boltzmann formulation of the Qian–Sheng [11] model of liquid crystals. However, the different viscosities in liquid crystals typically differ by at most a factor of five, while in a strongly magnetised plasma the perpendicular viscosity $\mu_{\perp}$ introduced in (10) below may be orders of magnitude smaller than $\mu_{\parallel}$.

2. The Boltzmann approach to hydrodynamics

The kinetic theory of dilute monatomic gases [5, 12, 13] uses a distribution function $f(\mathbf{x}, \boldsymbol{\xi}, t)$ to specify the number density of particles at position $\mathbf{x}$ and time t moving with velocity $\boldsymbol{\xi}$. The distribution function evolves according to the Boltzmann equation

$$\partial_t f + \boldsymbol{\xi}\cdot\nabla f = C[f, f], \tag{2}$$

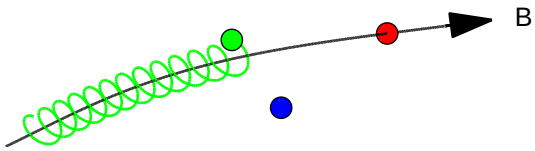

Figure 1: (Colour online.) A charged particle spiralling around a magnetic field line. Particles on the same field line interact more readily than particles on different field lines.

where $C[f, f]$ denotes a bilinear integral operator that describes binary collisions between particles. An example collision operator is given in (9) below. Collisions drive f towards a Maxwell–Boltzmann distribution,

$$f^{(0)} = \frac{\rho}{(2\pi\theta)^{3/2}} \exp\left(-\frac{|\boldsymbol{\xi} - \mathbf{u}|^2}{2\theta} \right), \tag{3}$$

while conserving mass, momentum, and energy. The parameters ρ, $\mathbf{u}$, and θ in $f^{(0)}$ will be defined below. This kinetic description is computationally attractive because $\boldsymbol{\xi}$ is an independent variable, so the left hand side of (2) is a *linear* differential operator. All nonlinearity is confined to the collision operator, which is local in $\mathbf{x}$ and t. However, this currently comes at the price of evolving f in a six-dimensional phase space.

Taking moments of (2) with respect to $\boldsymbol{\xi}$ leads to an infinite hierarchy of evolution equations for the moments of f. The first few of these are

$$\partial_t \rho + \nabla\cdot(\rho\mathbf{u}) = 0, \;\; \partial_t(\rho\mathbf{u}) + \nabla\cdot\boldsymbol{\Pi} = 0, \;\; \partial_t\boldsymbol{\Pi} + \nabla\cdot\mathsf{Q} = -\frac{1}{\tau}\left(\boldsymbol{\Pi} - \boldsymbol{\Pi}^{(0)}\right), \tag{4}$$

where the moments ρ, $\rho\mathbf{u}$, $\boldsymbol{\Pi}$, and Q are functions of $\mathbf{x}$ and t, as defined by

$$\rho = \int f d\boldsymbol{\xi}, \;\; \rho\mathbf{u} = \int \boldsymbol{\xi} f d\boldsymbol{\xi}, \;\; \boldsymbol{\Pi} = \int \boldsymbol{\xi}\boldsymbol{\xi} f d\boldsymbol{\xi}, \;\; \mathsf{Q} = \int \boldsymbol{\xi}\boldsymbol{\xi}\boldsymbol{\xi} f d\boldsymbol{\xi}. \tag{5}$$

These are the densities of mass (ρ), momentum ($\rho\mathbf{u}$), momentum flux ($\boldsymbol{\Pi}$), and energy flux (Q). The temperature θ (in energy units) is defined by $\mathrm{Tr}\boldsymbol{\Pi} = 3\rho\theta + \rho|\mathbf{u}|^2$. A superscript $^{(0)}$ denotes a moment of the equilibrium distribution $f^{(0)}$, such as $\boldsymbol{\Pi}^{(0)} = \int \boldsymbol{\xi}\boldsymbol{\xi} f^{(0)} d\boldsymbol{\xi}$.

The first two of equations (4) are conservation laws for mass and momentum. Their right hand sides vanish because mass and momentum are both conserved under collisions. However, they are not a closed system because the evolution of $\rho\mathbf{u}$ involves the higher moment $\boldsymbol{\Pi}$. The evolution of $\boldsymbol{\Pi}$ in turn involves the next higher moment Q, and so on. The evolution equation for $\boldsymbol{\Pi}$ also brings in a contribution from collisions. The simple form $-(1/\tau)(\boldsymbol{\Pi} - \boldsymbol{\Pi}^{(0)})$ occurs when $\boldsymbol{\Pi}$ is an eigenfunction of the collision operator, with eigenvalue $-1/\tau$. This holds exactly for the linearised Fokker–Planck collision operator for unmagnetised plasmas, and for the linearised Boltzmann collision operator for Maxwell molecules.

Hydrodynamics follows by seeking solutions to the system (4) that vary on a slow timescale T much longer than the collisional timescale τ. This is typically done using the Chapman–Enskog expansion [5, 12, 13], which may be formulated as a multiple scales expansion in the small parameter $\epsilon = \tau/T$,

$$\partial_t = \partial_{t_0} + \epsilon\partial_{t_1} + \cdots, \;\; \boldsymbol{\Pi} = \boldsymbol{\Pi}^{(0)} + \epsilon\boldsymbol{\Pi}^{(1)} + \cdots, \;\; \mathsf{Q} = \mathsf{Q}^{(0)} + \epsilon\mathsf{Q}^{(1)} + \cdots. \tag{6}$$

The quantities ρ and $\mathbf{u}$ that are conserved by collisions are left unexpanded. This is equivalent to imposing solvability conditions on an expansion of $f = f^{(0)} + \epsilon f^{(1)} + \cdots$. At leading order we obtain the compressible Euler equations in the form

$$\partial_{t_0}\rho + \nabla\cdot(\rho\mathbf{u}) = 0, \quad \partial_{t_0}(\rho\mathbf{u}) + \nabla\cdot\boldsymbol{\Pi}^{(0)} = 0, \tag{7}$$

where the inviscid momentum flux $\boldsymbol{\Pi}^{(0)} = \theta\rho\mathsf{I} + \rho\mathbf{u}\mathbf{u}$, with I the identity tensor, is given by the second moment of the Maxwell–Boltzmann distribution. Following a widely-used approximation in lattice Boltzmann hydrodynamics, we assume an isothermal fluid with constant temperature θ. In other words, we modify the collision operator so that temperature rather than energy is conserved under collisions. This approximation is valid when the Mach number $\mathrm{Ma} = |\mathbf{u}|/\sqrt{\theta}$ is small, and makes a separate energy equation redundant.

Evaluating the last of equations (4) at leading order yields an expression for the first correction $\boldsymbol{\Pi}^{(1)}$ to the momentum flux,

$$\partial_{t_0}\boldsymbol{\Pi}^{(0)} + \nabla\cdot\mathsf{Q}^{(0)} = -\frac{1}{T}\boldsymbol{\Pi}^{(1)}. \tag{8}$$

We may calculate $\mathsf{Q}^{(0)}$ from the known $f^{(0)}$, and we may evaluate $\partial_{t_0}\boldsymbol{\Pi}^{(0)}$ using the Euler equations (7). After some manipulation, $\epsilon\boldsymbol{\Pi}^{(1)} = -\tau\rho\theta\left[(\nabla\mathbf{u}) + (\nabla\mathbf{u})^{\mathsf{T}}\right]$ becomes the Navier–Stokes viscous stress in an isothermal fluid. We thus obtain the compressible Navier–Stokes equations with viscosity $\mu = \tau\rho\theta$ from the first two terms in the Chapman–Enskog expansion.

3. Kinetic theory of plasmas and Braginskii magnetohydrodynamics

The above derivation of hydrodynamic equations for a gas of uncharged particles gives an isotropic relation between the viscous stress $\mathbf{\Pi}^{(1)}$ and the strain rate. However, the analogue of equation (2) for charged particles in an electric field $\mathbf{E}$ and magnetic field $\mathbf{B}$ is [4]

$$\partial_t f + \boldsymbol{\xi}\cdot\nabla f + \frac{q}{m}\left(\mathbf{E} + \frac{\boldsymbol{\xi}\times\mathbf{B}}{c}\right)\cdot\frac{\partial f}{\partial\boldsymbol{\xi}} = \frac{2\pi q^4\ln\Lambda}{m^2}\frac{\partial}{\partial\boldsymbol{\xi}}\cdot\int\frac{\mathsf{I}-\hat{\mathbf{g}}\hat{\mathbf{g}}}{|\mathbf{g}|}\cdot\left[\frac{\partial f(\boldsymbol{\xi})}{\partial\boldsymbol{\xi}}f(\boldsymbol{\xi}') - \frac{\partial f(\boldsymbol{\xi}')}{\partial\boldsymbol{\xi}'}f(\boldsymbol{\xi})\right]d\boldsymbol{\xi}', \tag{9}$$

in the Gaussian electromagnetic units conventionally used in plasma physics. Here m and q are the mass and charge of the particles, c is the speed of light, $\mathbf{g} = \boldsymbol{\xi} - \boldsymbol{\xi}'$ is the relative velocity between colliding pairs of particles, and $\ln\Lambda$ is the Coulomb logarithm [4, 14]. The Landau form of the Fokker–Planck collision operator in (9) describes many glancing collisions mediated by Coulomb interactions.

Starting from two copies of (9) for separate ion and electron distribution functions, Braginskii [1] used a Chapman–Enskog expansion to derive hydrodynamic equations analogous to the Navier–Stokes equations, but for separate electron and ion fluids. Braginskii's equations are distinguished by their anistropic relations between stress and strain rate, and between electric field and current, with a preferred direction set by the magnetic field. Equivalent equations were later obtained by Balescu [15] using Grad's [16, 13] method of moments applied to the ion and electron kinetic equations. These "two-fluid" descriptions are more widely applicable than a single fluid description. Due to their widely differing masses, $m_\mathrm{i}/m_\mathrm{e} \approx 1836 \gg 1$, collisional energy transfers between ions and electrons are much slower than transfers between pairs of ions or pairs of electrons.

Nevertheless, a single fluid description, known as Braginskii MHD, is valid on sufficiently large and slow scales. Braginskii MHD resembles conventional resistive MHD apart from the use of Braginskii's anisotropic expressions for the dissipative terms. It is valid for motions with frequencies below the ion gyrofrequency $\Omega_\mathrm{i} = q|\mathbf{B}|/(m_\mathrm{i}\,c)$, and on length-scales larger than the ion gyroradius $v_\mathrm{th}/\Omega_\mathrm{i}$, where $v_\mathrm{th} = (T_\mathrm{i}/m_\mathrm{i})^{1/2}$ is the thermal velocity scale for ions at temperature T_i.

The incompressible limit of Braginskii MHD is an attractive theoretical model with astrophysical relevance [17], but the lattice Boltzmann approach requires a finite sound speed. We therefore assume an isothermal equation of state, as is common in lattice Boltzmann hydrodynamics, and a small Mach number. Moreover, the form (1) of the viscous stress is not quite satisfactory as written. The vanishing viscous stress perpendicular to the magnetic field leads to instabilities with arbitrarily large growth rates [17]. Braginskii MHD is therefore commonly regularised by changing the viscous stress to be

$$\mathbf{\Pi}_\mathrm{visc} = -\mu_\perp\mathbf{W} - (\mu_\parallel - \mu_\perp)\,\hat{\mathbf{b}}\hat{\mathbf{b}}\,\hat{\mathbf{b}}\hat{\mathbf{b}} : \mathbf{W}, \tag{10}$$

where $\mu_\perp$ is a small perpendicular viscosity, and $\mathbf{W} = \nabla\mathbf{u} + (\nabla\mathbf{u})^\mathsf{T}$ is the strain rate for an incompressible or isothermal fluid. One may also regularise (1) by including Braginskii's [1] perpendicular viscous stresses, which gives a viscosity ratio $\mu_\perp/\mu_\parallel \sim (\Omega_\mathrm{i}\tau_\mathrm{i})^{-2}$, where τ_i is the ion-ion collision time [4]. The two regularisations are equivalent for the flow studied below [18].

To summarise, we seek a lattice Boltzmann formulation of the isothermal, regularised form of Braginskii MHD,

$$\partial_t\rho = -\nabla\cdot(\rho\mathbf{u}), \tag{11a}$$

$$\rho(\partial_t\mathbf{u} + \mathbf{u}\cdot\nabla\mathbf{u}) = -\theta\nabla\rho + (4\pi)^{-1}(\nabla\times\mathbf{B})\times\mathbf{B} - \nabla\cdot\mathbf{\Pi}_\mathrm{visc}, \tag{11b}$$

$$\partial_t\mathbf{B} = \nabla\times(\mathbf{u}\times\mathbf{B}) + \eta_\perp\nabla^2\mathbf{B}. \tag{11c}$$

Solutions of these equations approach those of the incompressible Braginskii MHD equations as the Mach number $\mathrm{Ma} = |\mathbf{u}|/\sqrt{\theta} \to 0$, which is the typical lattice Boltzmann operating regime. Equation (11c) combines Faraday's law $\partial_t\mathbf{B}+\nabla\times\mathbf{E} = 0$ and Ohm's law in the form $\mathbf{E}+\mathbf{u}\times\mathbf{B} = \eta_\perp\nabla\times\mathbf{B}$ with resistivity $\eta_\perp$. It is common to ignore the distinction between parallel and perpendicular resistivities because $\eta_\perp = 1.96\eta_\parallel$, unlike the large disparity between $\mu_\perp$ and $\mu_\parallel$. Moreover, the current is perpendicular to the magnetic field in the computations below, so there is no inaccuracy in using $\eta_\perp$ throughout.

4. Lattice Boltzmann hydrodynamics

The lattice Boltzmann approach preserves the structure of continuum kinetic theory, as contained in (2) or (9), and of the derivation of hydrodynamics from kinetic theory. The chief difference, which leads to tractable numerical methods, is to restrict the particle velocity $\boldsymbol{\xi}$ to a discrete set $\boldsymbol{\xi}_0, \ldots, \boldsymbol{\xi}_{N-1}$. The distribution function $f(\mathbf{x}, \boldsymbol{\xi}, t)$ is replaced by a set of functions $f_i(\mathbf{x}, t)$, one for each $\boldsymbol{\xi}_i$, and integral moments are replaced by sums,

$$\rho = \textstyle\sum_i f_i,\ \rho\mathbf{u} = \sum_i \boldsymbol{\xi}_i f_i,\ \mathbf{\Pi} = \sum_i \boldsymbol{\xi}_i\boldsymbol{\xi}_i f_i,\ \mathsf{Q} = \sum_i \boldsymbol{\xi}_i\boldsymbol{\xi}_i\boldsymbol{\xi}_i f_i. \tag{12}$$

The analogue of the Boltzmann equation (2) is

$$\partial_t f_i + \boldsymbol{\xi}_i\cdot\nabla f_i = -\textstyle\sum_j \Omega_{ij}\,(f_j - f_j^{(0)}), \tag{13}$$

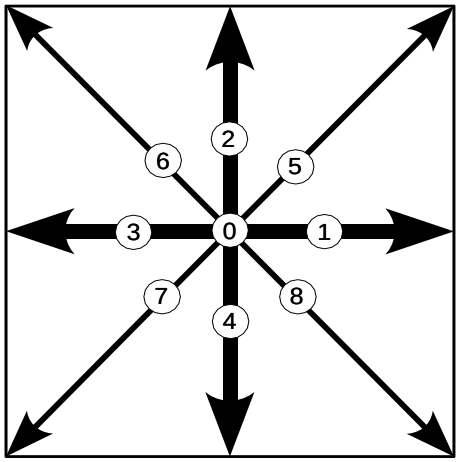

Figure 2: The nine particle velocities used in the hydrodynamic lattice Boltzmann scheme. Only the five velocities $0,\ldots,4$ shown in thicker lines are necessary for the magnetic field.

where the velocity space has been made discrete. The right hand side of (13) represents a general linear collision operator with an $N \times N$ collision matrix Ω_{ij}, and equilibrium distributions $f_j^{(0)}$.

The aim now is to choose the velocity set $\boldsymbol{\xi}_i$, the equilibria $f_i^{(0)}$, and the collision matrix Ω_{ij} so that the moment equations obtained from (13) exactly coincide with those obtained previously from (2). The discrete collision operator should conserve mass and momentum, and the momentum flux $\boldsymbol{\Pi}$ should be an eigenfunction. For example, the widely used Bhatnagar–Gross–Krook (BGK) collision operator [19] takes $\Omega_{ij} = (1/\tau)\delta_{ij}$, with equilibria [20]

$$f_i^{(0)} = \rho w_i \left(1 + \theta^{-1}\boldsymbol{\xi}_i \cdot \mathbf{u} + \tfrac{1}{2}\theta^{-2}(\boldsymbol{\xi}_i \cdot \mathbf{u})^2 - \tfrac{1}{2}\theta^{-1}|\mathbf{u}|^2\right). \tag{14}$$

The lattice constant θ is defined by $\sum_i w_i \boldsymbol{\xi}_i \boldsymbol{\xi}_i = \theta \mathsf{I}$. For the computations in this paper we used the particle velocities $\boldsymbol{\xi}_i$ that form the widely-used D2Q9 square lattice, as shown in figure 2. The corresponding weights are $w_0 = 4/9$, $w_{1,2,3,4} = 1/9$, and $w_{5,6,7,8} = 1/36$. Weights for this lattice, and also the D3Q15 and D3Q19 lattices, are given in [20].

5. A numerical scheme for hydrodynamics

Having shown that slowly varying solutions to the partial differential equations (13) obey the Navier–Stokes equations, we now discretise (13) in space and time to obtain a numerical scheme. The left hand side of (13) is a derivative along the characteristic defined by the particle velocity $\boldsymbol{\xi}_i$. Integrating (13) along this characteristic for a time step Δt therefore gives

$$f_i(\mathbf{x} + \boldsymbol{\xi}_i\Delta t, t + \Delta t) - f_i(\mathbf{x}, t) = -\textstyle\sum_j \Omega_{ij} \displaystyle\int_0^{\Delta t} f_j(\mathbf{x} + \boldsymbol{\xi}_i s, t + s) - f_j^{(0)}(\mathbf{x} + \boldsymbol{\xi}_i s, t + s) ds, \tag{15}$$

where the left hand side has been calculated exactly. Evaluating the integral on the right hand side by the trapezium rule leads to

$$\begin{aligned} f_i(\mathbf{x} + \boldsymbol{\xi}_i\Delta t, t + \Delta t) - f_i(\mathbf{x}, t) = -\tfrac{1}{2}\Delta t \textstyle\sum_j \Omega_{ij} \Big[& f_j(\mathbf{x} + \boldsymbol{\xi}_i\Delta t, t + \Delta t) \\ & - f_j^{(0)}(\mathbf{x} + \boldsymbol{\xi}_i\Delta t, t+\Delta t) + f_j(\mathbf{x}, t) - f_j^{(0)}(\mathbf{x}, t)\Big], \end{aligned} \tag{16}$$

after neglecting an $O(\Delta t^3)$ error. The implicitness caused by the terms evaluated at $t + \Delta t$ on the right hand side may be removed by introducing

$$\overline{f}_i(\mathbf{x}, t) = f_i(\mathbf{x}, t) + \tfrac{1}{2}\Delta t \textstyle\sum_j \Omega_{ij} \left(f_j(\mathbf{x}, t) - f_j^{(0)}(\mathbf{x}, t)\right). \tag{17}$$

Equation (16) then transforms into a system of algebraic equations [21, 22]

$$\overline{f}_i(\mathbf{x} + \boldsymbol{\xi}_i\Delta t, t + \Delta t) = \overline{f}_i(\mathbf{x}, t) - \Delta t \textstyle\sum_j \overline{\Omega}_{ij} (\overline{f}_j(\mathbf{x}, t) - f_j^{(0)}(\mathbf{x}, t)), \tag{18}$$

with a modified collision matrix given by $\overline{\boldsymbol{\Omega}} = \boldsymbol{\Omega}\,(\mathsf{I} + \frac{1}{2}\Delta t\,\boldsymbol{\Omega})^{-1}$. When $\Omega_{ij} = \tau^{-1}\delta_{ij}$, (17) and (18) reduce to the form given by He *et al.* [21].

$$\overline{f}_i(\mathbf{x} + \boldsymbol{\xi}_i\Delta t, t + \Delta t) - \overline{f}_i(\mathbf{x}, t) = -\frac{\Delta t}{\tau + \frac{1}{2}\Delta t} \left(\overline{f}_i(\mathbf{x}, t) - f_i^{(0)}(\mathbf{x}, t)\right). \tag{19}$$

The collision operator conserves mass and momentum, so we may reconstruct

$$\rho = \sum_i \overline{f}_i, \quad \rho\mathbf{u} = \sum_i \boldsymbol{\xi}_i \overline{f}_i, \tag{20}$$

from moments of the $\overline{f}_i$ instead of the f_i. We thus discard the f_i and evolve the $\overline{f}_i$ in time using (18). Equations (18) and (19) look like first-order accurate forward Euler approximations to the discrete Boltzmann PDE. They are in fact second-order accurate due to the transformation from f_i to $\overline{f}_i$.

6. Lattice Boltzmann approach for the magnetic field

We represent the magnetic field as $\mathbf{B} = \sum_i \mathbf{g}_i$ using a set of vector-valued distribution functions $\mathbf{g}_i$ that evolve according to the vector Boltzmann equation [9]

$$\partial_t \mathbf{g}_i + \boldsymbol{\xi}_i \cdot \nabla \mathbf{g}_i = -\frac{1}{\tau_m}\left(\mathbf{g}_i - \mathbf{g}_i^{(0)}\right). \tag{21}$$

This vector formulation is needed to obtain the curl in Faraday's evolution equation $\partial_t \mathbf{B} + \nabla\times\mathbf{E} = 0$ for the magnetic field. Using scalar distribution functions f_i leads to the vector moment $\rho\mathbf{u}$ evolving through the divergence of a *symmetric* tensor, while $\mathbf{B}$ evolves through the divergence of an *antisymmetric* tensor $\Lambda_{\alpha\beta} = -\epsilon_{\alpha\beta\gamma}E_\gamma$. Suitable equilibrium distributions are

$$\mathbf{g}_i^{(0)} = w_i\left[\mathbf{B} + \theta^{-1}\boldsymbol{\xi}_i \cdot (\mathbf{u}\,\mathbf{B} - \mathbf{B}\,\mathbf{u})\right]. \tag{22}$$

A Chapman–Enskog multiple-scales expansion of (21) leads to the correct evolution equation for the magnetic field under resistive magnetohydrodynamics,

$$\partial_t \mathbf{B} = \nabla\times(\mathbf{u}\times\mathbf{B}) + \nabla\cdot(\eta\nabla\mathbf{B}), \tag{23}$$

with constant resistivity η proportional to τ_m. Discretising (21) leads to a numeric scheme analogous to (19). This scheme preserves $\nabla\cdot\mathbf{B} = 0$ to round-off error [9]. It has been used in large-scale (up to 1800^3) simulations of three-dimensional MHD turbulence on parallel computers [23, 24], and in simulations of liquid metal flows relevant to cooling systems in nuclear reactors [25].

7. A collision operator for Braginskii magnetohydrodynamics

To simulate Braginskii MHD instead of isotropic resistive MHD we leave the magnetic part of the algorithm unchanged, but modify the hydrodynamic collision matrix Ω_{ij} so that the momentum flux $\boldsymbol{\Pi}$ evolves according to

$$\partial_t \boldsymbol{\Pi} + \nabla\cdot\mathsf{Q} = -\frac{1}{\tau_\parallel}\,\hat{\mathbf{b}}\hat{\mathbf{b}}\,\hat{\mathbf{b}}\hat{\mathbf{b}} : \left(\boldsymbol{\Pi} - \boldsymbol{\Pi}^{(0)}\right) - \left(\frac{1}{\tau_\parallel} - \frac{1}{\tau_\perp}\right)\left(\boldsymbol{\Pi} - \boldsymbol{\Pi}^{(0)}\right). \tag{24}$$

The evaluation of the left hand side under the Chapman–Enskog expansion is unchanged from before. The two relaxation times are $\tau_\parallel = \frac{1}{3}\mu_\parallel$ and $\tau_\perp = \frac{1}{3}\mu_\perp$ in the so-called lattice units with $\Delta x = \Delta t = 1$. This is most easily implemented by computing the post-collisional momentum flux $\overline{\boldsymbol{\Pi}}'$ using the discrete form of (24),

$$\overline{\boldsymbol{\Pi}}' = \overline{\boldsymbol{\Pi}} - \left(\overline{\boldsymbol{\Pi}} - \boldsymbol{\Pi}^{(0)}\right)\frac{\Delta t}{\tau_\perp + \frac{1}{2}\Delta t} - \hat{\mathbf{b}}\hat{\mathbf{b}}\,(\hat{\mathbf{b}}\hat{\mathbf{b}} : \overline{\boldsymbol{\Pi}} - \hat{\mathbf{b}}\hat{\mathbf{b}} : \boldsymbol{\Pi}^{(0)})\left(\frac{\Delta t}{\tau_\parallel + \frac{1}{2}\Delta t} - \frac{\Delta t}{\tau_\perp/\Delta t + \frac{1}{2}\Delta t}\right). \tag{25}$$

We write $\overline{\boldsymbol{\Pi}} = \sum_i \boldsymbol{\xi}_i\boldsymbol{\xi}_i\overline{f}_i$ for the second moment of the $\overline{f}_i$. This differs from $\boldsymbol{\Pi}$ because momentum flux is not conserved under collisions. The equilibrium momentum flux, including the Maxwell stress, is [9]

$$\boldsymbol{\Pi}^{(0)} = (\theta\rho + \tfrac{1}{2}|\mathbf{B}|^2)\mathsf{I} + \rho\mathbf{u}\mathbf{u} - \mathbf{B}\mathbf{B}. \tag{26}$$

The post-collisional distribution functions may then be reconstructed using

$$\overline{f}_i' = w_i\left[\rho\left(2 - \tfrac{3}{2}|\boldsymbol{\xi}_i|^2\right) + 3\rho\mathbf{u}\cdot\boldsymbol{\xi}_i + \tfrac{9}{2}\,\overline{\boldsymbol{\Pi}}' : \boldsymbol{\xi}_i\boldsymbol{\xi}_i - \tfrac{3}{2}\,\mathrm{Tr}\,\overline{\boldsymbol{\Pi}}'\right]. \tag{27}$$

The above happens locally at each grid point $\mathbf{x}$. To complete the timestep we propagate the post-collisional distribution functions to neighbouring grid points,

$$\overline{f}_i(\mathbf{x} + \boldsymbol{\xi}_i\Delta t, t + \Delta t) = \overline{f}_i'(\mathbf{x}, t). \tag{28}$$

The D2Q9 lattice has nine distribution functions, but there are only six independent degrees of freedom in ρ, $\mathbf{u}$, and $\overline{\boldsymbol{\Pi}}'$. The reconstruction (27) implicitly sets the extra degrees of freedom to zero. This is an example of the multiple relaxation time collision operators [22, 26] that have been used to improve stability in lattice Boltzmann simulations of isotropic MHD [25, 24]. By extending this idea further to apply different relaxation times to $\hat{\mathbf{b}}\hat{\mathbf{b}} : \boldsymbol{\Pi}$ and the other components of $\boldsymbol{\Pi}$ we may simulate Braginskii MHD as well as isotropic MHD.

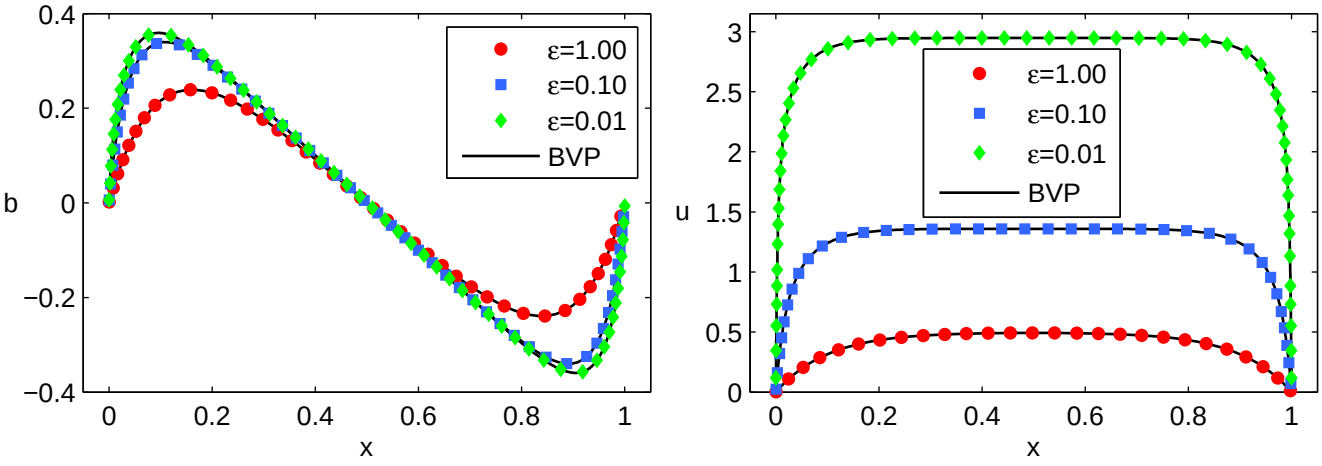

Figure 3: (Colour online.) Lattice Boltzmann computations (points) versus numerical solutions (lines) of the steady boundary value problem (BVP) for channel flow with Hartmann number Ha = 10 and three different values of the viscosity ratio $\epsilon = \mu_\perp/\mu_\parallel$.

8. Numerical experiments

We present some simulations of unidirectional flow in a channel spanned by a magnetic field. This is known as Hartmann flow, the MHD analogue of Poiseuille flow. The magnetic field across the channel is unaffected by the flow, but the flow generates a magnetic field along the channel, and hence a Lorentz force that resists the motion. No-slip and zero tangential magnetic field boundary conditions were imposed using the bounce-back rule on the hydrodynamic distribution functions, and bounce-back with sign reversal on the magnetic distribution functions, as in isotropic MHD [9]. This creates an effective boundary approximately half-way between grid points. The flow was forced by imposing an additional constant stress $F\hat{\mathbf{x}}\hat{\mathbf{y}}$ in $\mathbf{\Pi}^{(0)}$, as in previous computations [9]. This is equivalent to a body force $F\hat{\mathbf{y}}$ in the streamwise (y) momentum equation. Solutions to this problem are described by the dimensionless forcing strength $f = 4\pi FL/B_0^2$, the Hartmann number $\mathrm{Ha} = B_0 L(4\pi\eta_\perp\mu_\parallel)^{-1/2}$ and the viscosity ratio $\epsilon = \mu_\perp/\mu_\parallel$, where L is the channel width, and B_0 the magnitude of the applied field. Further details of the problem formulation, and the asymptotic form of its solutions for $\mathrm{Ha} \gg 1$ and $\epsilon \ll 1$, may be found in [18].

Figure 3 shows the computed streamwise velocity u and streamwise magnetic field b for $f = 1$ and $\mathrm{Ha} = 10$. The time-dependent simulations were run until they reached steady states. The peak velocity increases with decreasing viscosity ratio, due to the large shears that develop at the walls [18]. These results are in good agreement with steady solutions computed by the two-point boundary value problem solver TWPBVPC [27] with an error tolerance of 10^{-12} on an automatically generated mesh containing the fixed mesh used in the lattice Boltzmann computations as a subset. Figure 4 shows the ℓ_2 norms of the errors on these fixed meshes. Achieving second-order convergence with this driving force requires a reduction of the Mach number, and hence the timestep, in proportion to the grid spacing. This suppresses an error in the viscous stress due to the implementation of the body force driving the flow [9]. The simulations shown used $\mathrm{Ma} = \sqrt{3}/100$ for $N = 1024$ points. The asymptotic form of the steady solution has a maximum velocity proportional to $\epsilon^{-1/4}\,\mathrm{Ha}$, and boundary layers of width $\epsilon^{3/4}\,\mathrm{Ha}^{-1}$ on either wall [18]. The computations therefore become more demanding for larger Ha and smaller ϵ, both because more grid points are needed to resolve the boundary layers, and because a smaller timestep is needed to reduce the Mach number based on the peak velocity to a sufficiently small value.

9. Conclusions

Braginskii magnetohydrodynamics (MHD) is a single-fluid description of weakly collisional plasmas [1, 4]. The relation between stress and strain rate becomes highly anisotropic when the reciprocal ion gyrofrequency Ω_i^{-1} is much shorter than the ion-ion collision time τ_i. The effective mixing length perpendicular to magnetic fields lines is then much smaller than the mixing length parallel to the magnetic field.

We have adapted an earlier lattice Boltzmann formulation of isotropic MHD [9] to simulate Braginskii MHD in an isothermal, weakly compressible fluid. The key ingredient is an explicitly anistropic collision operator with a preferred direction set by the magnetic field. The Braginskii MHD equations may then be recovered from a Chapman–Enskog expansion, as in continuous kinetic theory. Preliminary computations show second-order convergence towards steady-state reference solutions. However, the solutions develop large velocities in narrow boundary layers on either wall, as predicted by analytical theory [18]. To reach larger Hartmann numbers and smaller viscosity ratios it would be beneficial to adopt the non-uniform meshes previously employed to resolve Hartmann layers in large-scale simulations of isotropic MHD [25].

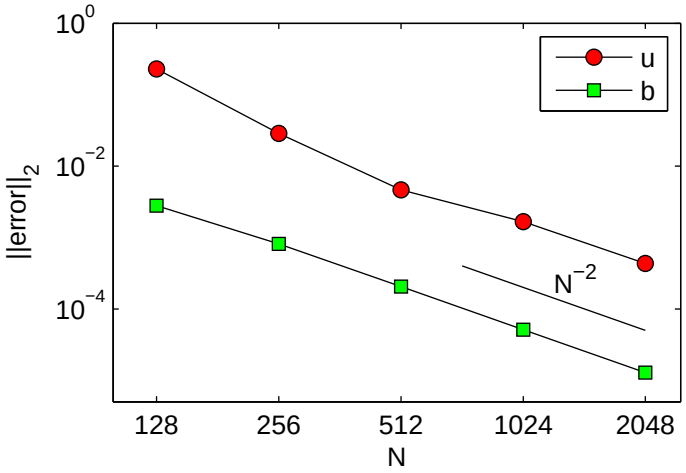

Figure 4: (Colour online.) Convergence to steady solutions under grid refinement for $f = 1$, Ha = 10, and $\epsilon = 0.01$. The errors in u are much larger due to the thin shear layers at the walls.

10. Role of the funding source

The author's research is supported by an Advanced Research Fellowship, grant number EP/E054625/1, from the UK Engineering and Physical Sciences Research Council. This body took no other part in the research, or in the preparation and submission of the manuscript.

References

[1] Braginskii, S.I.. Transport processes in a plasma. Rev Plasma Phys 1965;1:205–311.
[2] Lifshitz, E.M., Pitaevskii, L.P.. Physical Kinetics. Oxford: Pergamon; 1981.
[3] Balescu, R.. Transport Processes in Plasmas. Amsterdam; Oxford: North-Holland; 1988. 2 volumes.
[4] Kulsrud, R.M.. Plasma Physics for Astrophysics. Princeton, NJ: Princeton University Press; 2005.
[5] Chapman, S., Cowling, T.G.. The Mathematical Theory of Non-Uniform Gases. Cambridge: Cambridge University Press; 3rd ed.; 1970.
[6] Chen, S., Doolen, G.D.. Lattice Boltzmann method for fluid flows. Annu Rev Fluid Mech 1998;30:329–364.
[7] Succi, S.. The Lattice Boltzmann Equation: For Fluid Dynamics and Beyond. Oxford: Oxford University Press; 2001.
[8] Shan, X., Yuan, X.F., Chen, H.. Kinetic theory representation of hydrodynamics: a way beyond the Navier–Stokes equation. J Fluid Mech 2006;550:413–441.
[9] Dellar, P.J.. Lattice kinetic schemes for magnetohydrodynamics. J Comput Phys 2002;179:95–126.
[10] Care, C.M., Halliday, I., Good, K., Lishchuk, S.V.. Generalized lattice Boltzmann algorithm for the flow of a nematic liquid crystal with variable order parameter. Phys Rev E 2003;67:061703–10.
[11] Qian, T., Sheng, P.. Generalized hydrodynamic equations for nematic liquid crystals. Phys Rev E 1998;58:7475–7485.
[12] Cercignani, C.. The Boltzmann Equation and its Applications. New York: Springer-Verlag; 1988.
[13] Grad, H.. Principles of the kinetic theory of gases. In: Flügge, S., editor. Thermodynamik der Gase; vol. 12 of *Handbuch der Physik*. Berlin: Springer-Verlag; 1958, p. 205–294.
[14] Spitzer, L.. Physics of Fully Ionized Gases. New York: Wiley; 1962.
[15] Balescu, R.. Transport Processes in Plasmas: Classical Transport Theory. Amsterdam; Oxford: North-Holland; 1988.
[16] Grad, H.. On the kinetic theory of rarefied gases. Comm Pure Appl Math 1949;2:331–407.
[17] Schekochihin, A., Cowley, S., Kulsrud, R., Hammett, G., Sharma, P.. Magnetised plasma turbulence in clusters of galaxies. In: Chyzy, K.T., Otmianowska-Mazur, K., Soida, M., Dettmar, R.J., editors. The Magnetized Plasma in Galaxy Evolution. Jagiellonian University, Kracow, Poland; 2005, p. 86–92.
[18] Dellar, P.J.. Planar channel flow in Braginskii magnetohydrodynamics. J Fluid Mech 2010,in press, doi:10.1017/S0022112010004507.
[19] Bhatnagar, P.L., Gross, E.P., Krook, M.. A model for collision processes in gases. I. Small amplitude processes in charged and neutral one-component system. Phys Rev 1954;94:511–525.
[20] Qian, Y.H., d'Humières, D., Lallemand, P.. Lattice BGK models for the Navier–Stokes equation. Europhys Lett 1992;17:479–484.
[21] He, X., Chen, S., Doolen, G.D.. A novel thermal model of the lattice Boltzmann method in incompressible limit. J Comput Phys 1998;146:282–300.
[22] Dellar, P.J.. Incompressible limits of lattice Boltzmann equations using multiple relaxation times. J Comput Phys 2003;190:351–370.
[23] Vahala, G., Keating, B., Soe, M., Yepez, J., Vahala, L., Carter, J., et al. MHD turbulence studies using lattice Boltzmann algorithms. Commun Comput Phys 2008;4:624–646.
[24] Riley, B., Richard, J., Girimaji, S.S.. Assessment of magnetohydrodynamic lattice Boltzmann schemes in turbulence and rectangular jets. Int J Mod Phys C 2008;19:1211–1220.
[25] Pattison, M., Premnath, K., Morley, N., Abdou, M.. Progress in lattice Boltzmann methods for magnetohydrodynamic flows relevant to fusion applications. Fusion Eng Design 2008;83:557–572.
[26] d'Humières, D., Ginzburg, I., Krafczyk, M., Lallemand, P., Luo, L.S.. Multiple-relaxation-time lattice Boltzmann models in three dimensions. Phil Trans R Soc Lond A 2002;360:437–451.
[27] Cash, J.R., Mazzia, F.. A new mesh selection algorithm, based on conditioning, for two-point boundary value codes. J Comput Appl Math 2005;184:362–381.